

Electrophysiological evidence for linear polarization sensitivity in the compound eyes of the stomatopod crustacean *Gonodactylus chiragra*

Sonja Kleinlogel* and N. Justin Marshall

Vision Touch and Hearing Research Centre, School of Biomedical Sciences, University of Queensland, Brisbane QLD 4072, Australia

*Author for correspondence (e-mail: S.Kleinlogel@uq.edu.au)

Accepted 8 August 2006

Summary

Gonodactyloid stomatopod crustaceans possess polarization vision, which enables them to discriminate light of different e-vector angle. Their unusual apposition compound eyes are divided by an equatorial band of six rows of enlarged, structurally modified ommatidia, the mid-band (MB). The rhabdoms of the two most ventral MB rows 5 and 6 are structurally designed for polarization vision. Here we show, with electrophysiological recordings, that the photoreceptors R1–R7 within these two MB rows in *Gonodactylus chiragra* are highly sensitive to linear polarized light of two orthogonal directions (PS=6.1). They possess a narrow spectral sensitivity peaking at 565 nm. Unexpectedly, photoreceptors within the distal rhabdomal tier of MB row 2 also possess highly sensitive linear

polarization receptors, which are in their spectral and polarization characteristics similar to the receptors of MB rows 5 and 6. Photoreceptors R1–R7 within the remainder of the MB exhibit low polarization sensitivity (PS=2.3). Outside the MB, in the two hemispheres, R1–R7 possess medium linear polarization sensitivity (PS=3.8) and a broad spectral sensitivity peaking at around 500 nm, typical for most crustaceans. Throughout the retina the most distally situated UV-sensitive R8 cells are not sensitive to linear polarized light.

Key words: underwater polarization vision, photoreceptor, compound eye, retina, e-vector, communication.

Introduction

Many invertebrate photoreceptors are inherently sensitive to polarized light because of the dichroism of their rhabdomeres (Waterman, 1966; Waterman, 1981). Polarization vision, as opposed to polarization sensitivity (PS) of the retina, is the ability to discriminate between two lights of the same luminous intensity but of different e-vector orientation (Φ) and/or degree of polarization (Kirschfeld, 1973). Behavioural experiments have shown that gonodactyloid stomatopods possess polarization vision as they can discriminate two light sources on the basis of Φ (Marshall et al., 1999).

Gonodactyloid stomatopods of the species *Gonodactylus chiragra* are typically found in rocky inshore habitats in the low intertidal zone, where they are exposed to high light intensity (Caldwell and Dingle, 1976). Here, close to the water surface, the polarization pattern of the sky can still be seen within Snell's window (Horváth and Varjú, 2004). Outside this aerial window, the polarized light field produced by scattering and reflectance within the water itself is predominantly horizontal and therefore provides a predictable background (Cronin and Shashar, 2001; Waterman, 1981). These relatively consistent environmental stimulus conditions favour the evolution of underwater polarization vision, the most general function of which is

contrast enhancement (Bernard and Wehner, 1977). However, polarization vision is probably also used for tasks such as communication (Lythgoe, 1971; Lythgoe, 1979; Lythgoe and Hemmings, 1967; Shashar et al., 2000; Shashar et al., 1998). Many stomatopod species possess polarized body markings which, like colour signals, are displayed in behavioural contexts that seem clearly linked to intraspecific signalling (Cronin et al., 2004; Cronin et al., 2003).

The stalked apposition compound eyes of gonodactyloid stomatopods are subdivided into a dorsal and a ventral hemisphere bisected by an equatorial band of six distinct rows of enlarged ommatidia, termed the mid-band (MB; Fig. 1). The structure of the fused rhabdoms in both, the MB and the hemispheres is based on a two-tiered design, typical of many crustaceans (Nässel, 1976; Strausfeld and Nässel, 1981). There is a relatively short 8th retinula cell (R8 cell) as the top tier, and this overlies a longer tier, the main rhabdom, constructed by retinula cells R1–R7 (Fig. 2A). In the hemispheres and MB rows 5 and 6, the R1–R7 cells contribute to the entire length of the main rhabdom, whereas in MB rows 1–4 this main rhabdom is subdivided into a distal (D) and a proximal (P) tier (Fig. 2). The MB rows will hereafter be referred to simply as 'rows'.

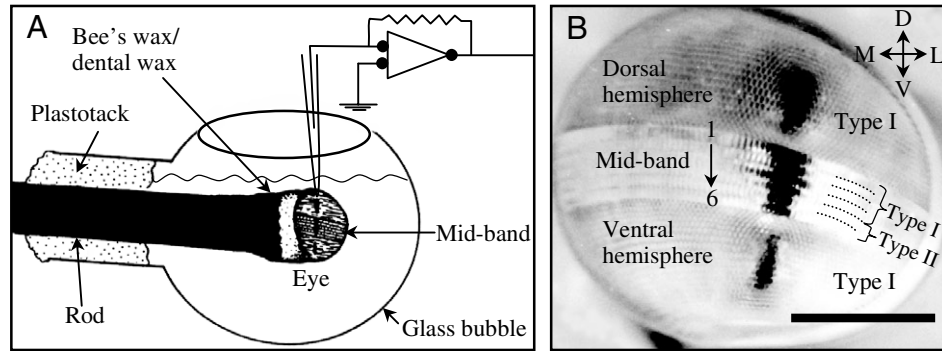


Fig. 1. Preparation. (A) The isolated apposition compound eye was mounted on a plastic rod with the aid of low melting point bee's wax/dental wax and placed into a glass bubble filled with saline so that the mid-band was oriented horizontally. The intracellular electrode was lowered through a small hole cut into the cornea of the dorsal (or ventral) hemisphere. (B) Frontal view of a left eye of *Gonodactylus chiragra* mounted as in A. The eye is divided into a dorsal and a ventral hemisphere by an equatorial mid-band formed by six rows of enlarged ommatidia. The mid-band rows are numbered 1 to 6 from dorsal to ventral. Ommatidia in rows 1–4 belong to type II, whereas ommatidia in rows 5 and 6 belong to type I (see Fig. 2). D, dorsal; V, ventral; L, lateral; M, medial. Scale bar, 1 mm.

In the hemispheres and rows 5 and 6, the R1–R7 cells are subdivided into two groups (Group I and Group II), which form layers of orthogonal microvilli (Fig. 2A). Group I cells, labelled R1, R4 and R5, have their microvilli at right angles to the microvilli of Group II cells, labelled R2, R3, R6 and R7 (Marshall et al., 1991a). Photoreceptors of the two groups are therefore expected to be sensitive to orthogonal e-vector orientations of light (Waterman, 1981). In rows 5 and 6 the microvilli within each cell group possess an especially high degree of alignment and the microvillar layers are only 5–6 microvilli deep (Fig. 2A). This precise arrangement suggests

increased linear PS in these rows compared to hemispheric receptors, where the microvillar layers are 8–9 microvilli deep and less crystalline in arrangement (Marshall et al., 1991a; Snyder, 1973; Stowe, 1983). In contrast, the individual photoreceptors of rows 1–4 produce microvilli in both orthogonal directions, as do R8 cells (Marshall et al., 1991a). The microvillar layers are here uneven and disorganized, which theoretically decreases PS drastically. In rows 1–4 Group I and Group II photoreceptors form separate rhabdomal tiers (Fig. 2) and are sensitive to different wavelengths of light. The total of eight spectral sensitivities within the main rhabdoms of MB

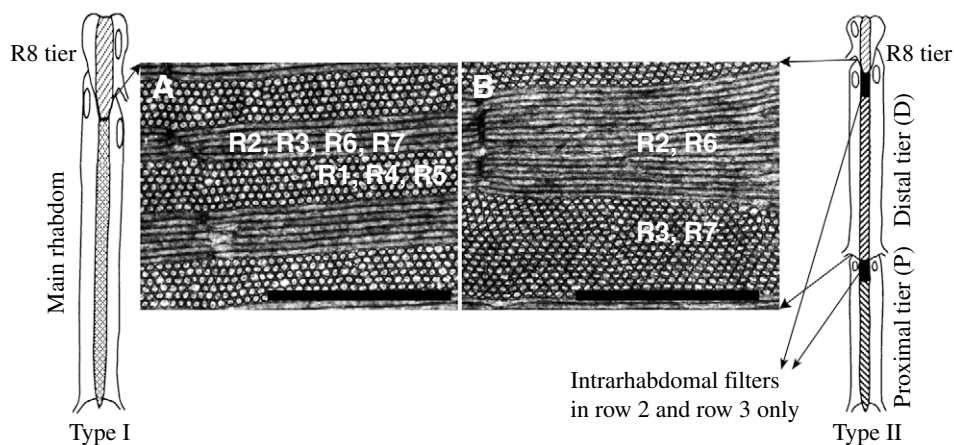


Fig. 2. The two rhabdom types within the retina. Type I (left) is found in mid-band rows 5 and 6 and both hemispheres, whereas type II (right) is only found in MB rows 1–4. Each rhabdom has a distally placed eighth retinula cell (R8) that overlies the main rhabdom composed of microvilli from retinula cells 1–7 (R1–R7). The R1–R7 cells are divided into two groups (Group I and Group II). In type I rhabdoms, R1–R7 contribute to the entire length of the main rhabdom and Group I (R1, R4, R5) and Group II (R2, R3, R6, R7) cells form mutually perpendicular, regular layers of microvilli. (A,B) Longitudinal electron microscopic sections through the main rhabdoms. (A) A row 5 rhabdom, which has very thin layers (5–6 microvilli deep) of orthogonal microvilli. In type II rhabdoms, the R1–R7 form two separate rhabdomal tiers, a distal (D) and a proximal (P) tier. The type II rhabdom is therefore three-tiered. In rows 1, 2P, 3 and 4 the microvilli within the rhabdoms are unordered, because each retinula cell produces microvilli in both orthogonal directions. (B) Rhabdom 2D is an exception. Here the four cells forming the rhabdom are also divided into 2 subgroups (R2, R6 and R3, R7), which form orthogonal layers of microvilli. However, the microvillar layers are about three times thicker (16–17 microvilli deep) than the layers found in rows 5 and 6. Scale bars, 2 μm .

rows 1–4 covers the spectrum from 400 nm to 725 nm continuously and the UV range down to 300 nm is included via the overlying R8 cells (Cronin and Marshall, 1989a; Cronin and Marshall, 1989b; Cronin et al., 1994b; Marshall and Oberwinkler, 1999). Rows 2 and 3 are equipped with long-pass coloured filters between the rhabdomal tiers (intrarhabdomal filters) in order to shift their spectral sensitivities to longer wavelengths (Fig. 2) (Marshall et al., 1991b). Owing to this diversity in spectral sensitivity it was proposed that photoreceptors within rows 1–4 are involved in colour vision and they will hereafter be referred to as ‘colour receptors’.

Many insects are equipped with a specialized retinal area for polarization vision, the so-called dorsal rim area. In general, crustaceans lack such a specialized area for polarization vision and their inherently polarization sensitive photoreceptors are distributed homogeneously across the retina (Eguchi and Waterman, 1966; Shaw, 1966; Waterman and Fernandez, 1970). This study shows an exception to the general rule. Although *Gonodactylus chiragra* possesses ‘typical crustacean’ polarization receptors in both hemispheres, we found specialized polarization receptors with a much higher PS exclusively in rows 2D, 5 and 6 of the MB. They will hereafter be referred to as ‘high PS cells’. The ‘high PS cells’ are sensitive to two orthogonal e-vector directions of polarized light and their narrow spectral sensitivities peaking at 565 nm are well suited to detect polarized body markings displayed by a variety of stomatopod species (Cronin et al., 2004; Cronin et al., 2003).

Materials and methods

Animals

Adult male and female stomatopods of the species *Gonodactylus chiragra* Fabricius 1781 (Crustacea, Hoplocarida, Stomatopoda, Gonodactyloidea) were collected at low tide from their burrows in the beach rock on Heron Island (Queensland–GBRMPA permit # G00/023) and maintained under a 12 h:12 h dark:light cycle in marine aquaria as approved by AQIS (Australian Quarantine Inspection Service) and Environment Australia Wildlife Protection. Overhead lighting was from UV-enhanced fluorescent light sources (‘TL’D natural light and Blacklight) directly above the tanks. Animals were cooled on ice before the eyes were removed and then killed by decapitation. All procedures were approved by the Animal Ethics Committee (UAEC, permit # 463/04) of the University of Queensland.

Stimulation

The light stimulus was produced by a 150 W xenon-arc lamp (Oriel, Stratford, USA) in combination with a computer-controlled monochromator (Oriel, Stratford, USA). A slit-width of 1.24 mm was used, which produced light of a spectral composition with approximately 4 nm halfwidth (information given by Oriel). The grating of the monochromator could be bypassed by a front-surface-mirror in order to provide white light. The light beam was first passed through a circular,

computer-controlled neutral density wedge (Edmund Optics, Barrington, USA) for intensity variations covering a range of four log units and then through an electronic shutter (Melles-Griot, New York, USA). The light was focused into a flexible UV-transmitting liquid light-guide, the other end of which was mounted on a cardan arm perimeter device, providing a stimulus of 0.9° for a stomatopod eye mounted in the centre of the arrangement. The cardan arm arrangement allowed adjustment of the angular position of the light stimulus around the preparation, yet maintained a fixed distance between eye and stimulus. Between the end of the light guide and the eye a broad-band (350 nm–750 nm) grey ($ND \approx 0.2$) linear polarization filter (27340 Polarizer, Oriel, Stratford, USA) could be inserted and its angle relative to the eye changed in 10° steps. The transmission of the optical system was calibrated with an USB 2000 spectrometer (Ocean Optics, Dunedin, Florida, USA), which was itself calibrated against a secondary NIST standard lamp (Oriel, Stratford, USA). At the location of the eye the white light had an unattenuated maximal intensity of approximately 10^{18} photons $s^{-1} cm^{-2}$ and the degree of polarization of the stimulus with the linear polarization filter in place exceeded 98% over the spectral range from 400 nm to 720 nm.

Preparation and recording

An eye was mounted on a plastic rod with the help of a low-melting-point bee’s wax/dental wax mixture (kindly supplied by S. B. Laughlin). A small hole (about five facets across) was cut with a razor blade in either the dorsal or the ventral hemisphere, the rod was then placed in a glass bubble filled with stomatopod saline (Watanabe et al., 1967), which was placed at the centre of the cardan arm arrangement with the MB oriented horizontally (Fig. 1A). A microelectrode was lowered vertically through the corneal hole and into the retina. The entire procedure was performed under photographic safelight to avoid excessive light adaptation of photoreceptors.

Photoreceptors were impaled using thick-walled borosilicate microelectrodes either filled with 1 mol l^{-1} KCl (40–100 M Ω) or 5% Lucifer Yellow CH (Sigma-Aldrich Pty Ltd, Castle Hill, NSW, Australia) in 0.1 mol l^{-1} Tris buffer and 1 mol l^{-1} LiCl (150–300 M Ω). The pipette was connected to the headstage of an intracellular amplifier (Axoprobe 1A, Axon Instruments Ltd, Inverurie, Scotland) via a chloride silver electrode and an Ag/AgCl pellet immersed in saline served as ground electrode. The amplified intracellular signals from photoreceptors were monitored on a digital oscilloscope (Tektronix, Brighton, East Sussex, UK).

Experimental protocol and evaluation of data

Upon impalement of the photoreceptor, the photoreceptor was activated with short flashes of white light and the light source was approximately aligned with its optical axis by moving it to the position that elicited maximal response. Only photoreceptors with a response of at least 30 mV to white light were investigated further. First the photoreceptor was characterized by its spectral sensitivity, which was measured

using the spectral scan method (Menzel et al., 1986). In this method, a photoreceptor is clamped to a preselected DC potential (criterion response) by adjusting the light flux *via* the neutral density wedge (ND) during changes in spectral content as delivered by the monochromator. The spectral sensitivity function $S(\lambda)$ of the cell is given by the reciprocal of the number of quanta of each wavelength required to maintain the criterion depolarization (Menzel, 1979). At least three scans with varying criterion responses were recorded for each photoreceptor and averaged. The analysis was performed using ASYST software (Keithley Instruments Inc., Cleveland, Ohio, USA).

To assess polarization sensitivity, short (50 ms) equal-quanta flashes of white light (the monochromator grating replaced with the front-surface mirror) with an interstimulus interval of 10 s were presented to the photoreceptor while the linear polarizer was given one full 360° turn in 20° steps (Fig. 3A,B). Responses at which polarization sensitivity was computed were always well above threshold and well below saturation. Response saturation actually never occurred, even at the brightest light intensity, possibly indicating that the photoreceptor response range is matched to the high light intensities found in shallow coral reefs. The two polarizer angles that elicited maximal (Φ_{\max}) and minimal (Φ_{\min}) response, respectively, were then determined more accurately by a second run in which the polarizer was turned in steps of 10° around the maximum ($\Phi_{\max}-20^\circ$, $\Phi_{\max}-10^\circ$, Φ_{\max} , $\Phi_{\max}+10^\circ$, $\Phi_{\max}+20^\circ$) and the minimum ($\Phi_{\min}-20^\circ$, $\Phi_{\min}-10^\circ$, Φ_{\min} , $\Phi_{\min}+10^\circ$, $\Phi_{\min}+20^\circ$). From previous anatomical investigations it was assumed that all data fall into groups at +45, -45, 90 and 0 degrees (Marshall et al., 1991a) and Φ_{\max} and Φ_{\min} were therefore allocated to one of the above anatomical groups. Two response-intensity (R -log I) functions were then recorded by applying 0.25 log intensity series of flashes of white light. The first R -log I function was recorded with the polarizer positioned in the direction found to generate

maximal response (Φ_{\max}) and a second curve with light polarized in the perpendicular direction (Φ_{\min}), which elicited minimal response (Fig. 3C). No baseline shift was allowed between the two R -log I function measurements. Single photoreceptor responses were digitised on a virtual oscilloscope (ADC-100) using Pico Scope software (Pico Technology, Camperdown, NSW, Australia) and then exported into Excel for analysis. All R -log I curves were fitted to standard Rushton intensity-response functions (Naka and Rushton, 1966a; Naka and Rushton, 1966b) using SigmaPlot 5.01 software (Systat Software, Hounslow, London, UK). Polarization sensitivity (PS) is defined as the ratio between maximal and minimal sensitivity of the photoreceptor to e-vector orientation and can be determined from the intensity

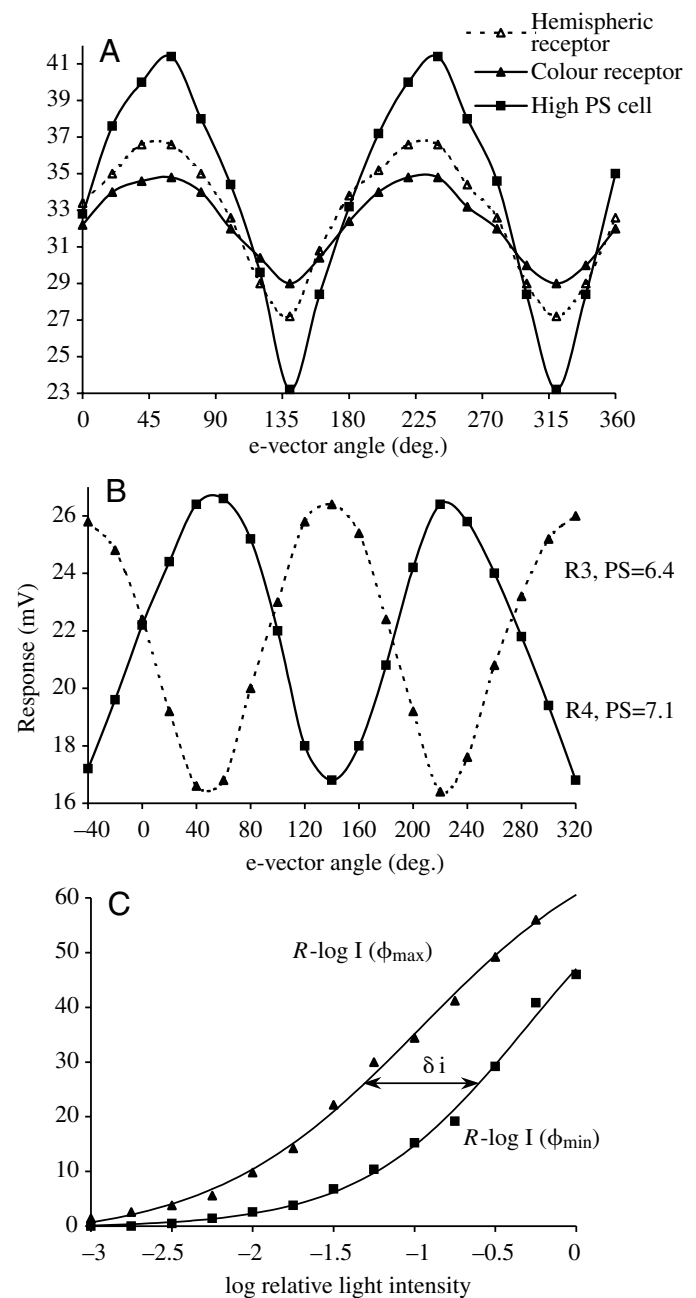


Fig. 3. (A) Comparison of the e-vector angle–response amplitudes of a colour receptor (row 4P R6), a hemispheric receptor (DH R1) and a ‘high PS cell’ (row 2D R2). All photoreceptors shown here possess similar response amplitudes to unpolarized white light, and nearly parallel response-intensity (R -log I) functions. They are all most sensitive to an e-vector orientation of linearly polarized light (Φ_{\max}) of approximately +45°. (B) Intracellular recordings of the e-vector angle–response curves of two neighbouring photoreceptors (R3 and R4) within row 5. The two cells possess 90° phase-shifted Φ_{\max} ($\Phi_{\max(R4)}=+45^\circ$ and $\Phi_{\max(R3)}=-45^\circ$). Slight re-positioning of the microelectrode after completing the recording and staining of the first cell (R3) resulted in a 90° phase-shift of Φ_{\max} . Subsequent Lucifer Yellow injection showed that the microelectrode tip had moved from R3 into the neighbouring retinula cell R4. R4 belongs to Group I and R3 to Group II cells amongst R1–R7, and they have their microvilli arranged at right angles. (C) To determine the polarization sensitivity of a photoreceptor, two R -log I curves were recorded at Φ_{\max} and Φ_{\min} , respectively. In this example, the intensity shift (δi) of 0.72 log units between the linear parts of the two fitted standard Rushton intensity-response functions corresponds to a polarization sensitivity of 5.2.

shift δi between the two fitted R -log I curves (Fig. 3C) (Dacke et al., 2002):

$$PS=10^{\delta i}$$

It is important to note that PS was probably slightly underestimated in some recordings because the minimal angle the polarizer could be turned was 10° and Φ_{\max} and Φ_{\min} were therefore determined with an accuracy of only $\pm 5^\circ$. However, e-vector-response curves are approximated sine-curves, which flatten around their minimum and maximum. The inaccuracy of Φ_{\max} and Φ_{\min} would result in a PS for example of 3.2 (6.0) instead of 3.5 (7.1), which does not influence the qualitative findings of this study.

At the end of each recording some cells were iontophoretically marked with Lucifer Yellow CH (Sigma Aldrich Pty Ltd, Castle Hill, NSW, Australia) using a 0.2 to 0.7 nA hyperpolarizing DC current at 1 Hz for 8 min.

Histology

Eyes were fixed in 4% paraformaldehyde and 30% sucrose in 0.1 mol l^{-1} phosphate buffer for 2–3 days at room temperature. The tissue was dehydrated in ethanol and embedded in 2-hydroxyethylmethacrylate (Technovit T7100, Heraeus, Germany). Serial frontal sections of $7 \mu\text{m}$ thickness were then cut on a historange microtome (LKB) and viewed under a Zeiss Axioscope microscope equipped with a digital SPOT camera using fluorescent microscopy and ALPHA Vivid standard Lucifer Yellow XF14 filters (Omega Optical, Inc., Brattleboro, VT, USA). Images were processed and the contrast enhanced using Adobe Photoshop 7.0 (Adobe Systems).

Results

The polarization and spectral sensitivities of 76 photoreceptors of 23 male and female stomatopods of the species *Gonodactylus chiragra* were measured (for an overview see Table 1). No noticeable discrepancy was found between male and female animals. Thirty-three of these cells were successfully stained with Lucifer Yellow, which clearly identified the photoreceptor from its position within the ommatidium (Marshall et al., 1991a) when observed in serial light microscopic sections through the retina (Fig. 4B). The spectral characteristics of the stained photoreceptors and the order of impalement by the electrode were used to identify cells that have not been stained.

Polarization sensitivity

Stomatopod photoreceptors can be divided into four groups according to their PS and anatomical position (Fig. 3A, Fig. 5). Thereby we assumed that within each ommatidial row, photoreceptors of the same cell group (R8; Group I, Group II) are identical in terms of their physiological properties (for an overview see Table 2). An exception is row 2D, which will be commented on later.

Lucifer Yellow injections confirmed that the UV-sensitive photoreceptors are R8 cells (Marshall and Oberwinkler, 1999). All UV-sensitive cells ($N=17$) exhibited negligible PS values of <2 . None of the R8 receptors of rows 5 and 6 was stained and it thus remains unclear if our results include any recording from these cells. Rows 5 and 6 R8 cells are of interest because they form unidirectional microvilli and PS is therefore expected (Marshall et al., 1991a). The photoreceptors of the dorsal and ventral hemispheres, which have a 'typical crustacean' design,

Table 1. Overview of recordings

Eye area	Total recordings (number stained)	Φ_{\max} (cell identity)		Stained cells	
		$+45^\circ$	-45°	R1,4,5	R2,3,6,7
High PS cells	14 (5)				
Row 2D		2 (R2, R6)	4 (R3, R7)	3 (2×R7, R6)	
Rows 5 and 6		5 (row 5: R2, R3, R6, R7) 5 (row 6: R1, R4, R5)	3 (row 5: R1, R4, R5) 3 (row 6: R2, R3, R6, R7)	1 (row 6: R3)	1 (row 5: R7)
Colour receptors	22 (12)				
Row 1		2	4	3	1
Row 2P		1	3	1	1
Row 3		3	1	2	1
Row 4		6	2	2	1
UV receptors	17 (9)				
Hem R8		10	7		3
Rows 1–4 R8					6
Rows 5 and 6 R8			?		0
Hemispheric receptors	17 (7)				
DH		5 (R1, R4, R5)	4 (R2, R3, R6, R7)	2	2
		90°	Φ_{\max}		
VH		5 (R1, R4, R5)	3 (R2, R3, R6, R7)	1	2
			0°		

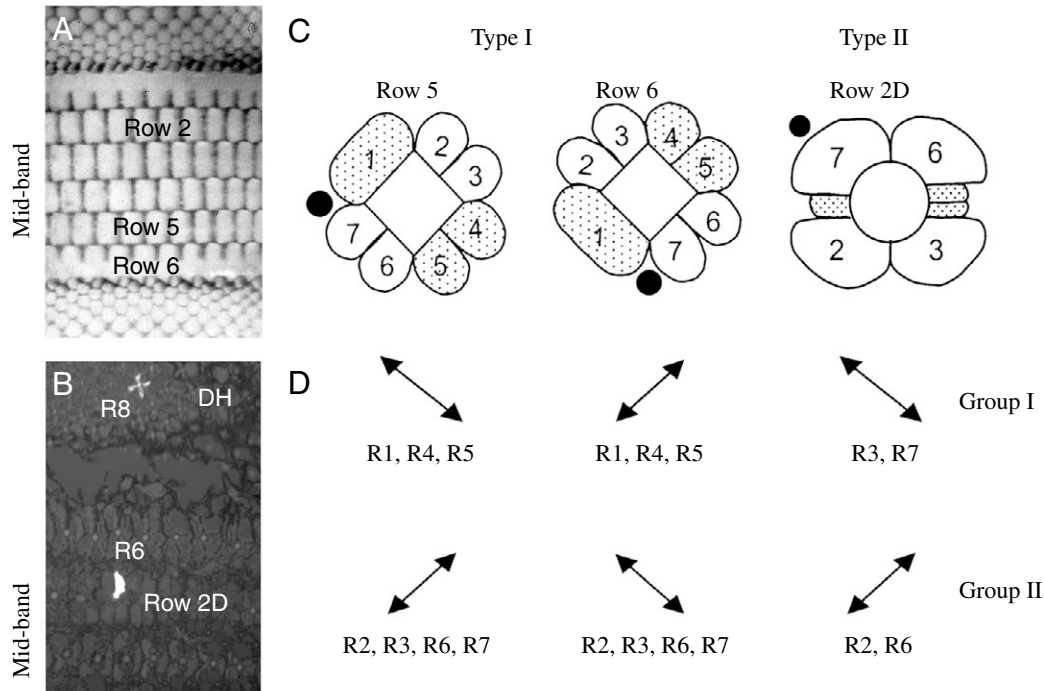


Fig. 4. (A) Photomicrograph of the mid-band region of the cornea. 'High PS cells' are found within rows 2D, 5 and 6. (B) 7 μm frontal section through the retina showing a dye-filled R8 cell of the dorsal hemisphere (DH) and a R6 cell of row 2D. (C) Diagrams of the arrangement of retinula cells R1–R7 in rows 2D, 5 and 6 in a right eye (frontal view). Group I retinula cells are stippled and Group II retinula cells are plain. Note that the cell arrangement in row 6 is twisted 90° counterclockwise compared to row 5 as identified by the R8 axon position, the dark spot. (D) Preferred e-vector orientations (Φ_{max}) of the two retinula cell groups (Group I and Group II). The Φ_{max} of the two cell groups are perpendicular and coincide with the microvillar orientations within the corresponding photoreceptors. Row 2D (distal rhabdomal tier) is formed by only four retinula cells, which are also divided into two cell groups sensitive to orthogonal Φ_{max} (R2, R6 and R3, R7). See Marshall et al. (Marshall et al., 1991a) for anatomical details.

had an average PS of 3.8 ± 1.6 (mean \pm s.d., $N=17$). The colour receptors, as expected from structure, had generally small PS values of 2.3 ± 1 ($N=22$). However, individual photoreceptors within row 2D were an exception. They had PS values of 6.2 ± 1.3 ($N=6$), significantly higher (t -test, $P < 0.01$) than the PS values measured for any other 'colour receptor', including row 2P receptors. The PS values of 2D receptors equalled the high PS values measured for photoreceptors of rows 5 and 6, which are 6.7 ± 2.5 ($N=8$). Therefore photoreceptors of rows 2D, 5 and 6 are hereafter grouped together as 'high PS cells' with an average PS of 6.1 ± 2 ($N=14$). 'High PS cells' are significantly more sensitive to polarized light than hemispheric receptors (t -test, $P < 0.005$).

Re-examination of electron microscopic investigations of the structure of rhabdom 2D revealed that the microvilli in this rhabdom are more organized than in the other row 1–4 rhabdoms. In row 2D each photoreceptor almost certainly produces microvilli in only one direction and the orthogonal layers are of equal thickness, albeit three times thicker (16–17 microvilli deep) than in rows 5 and 6 (see Fig. 2B). Both structural observations indicate PS of photoreceptors within row 2D. This is the only MB 1–4 row where four cells are present in the distal tier, suggesting a potential functional difference.

Spectral sensitivity

Photoreceptors of the dorsal and the ventral hemispheres produced broad spectral sensitivity curves with peak sensitivities between 450 nm and 550 nm. Although the averaged spectral sensitivity curves of dorsal and ventral hemisphere photoreceptors peak at different wavelengths, they cover the same spectral range with a similar sensitivity distribution and they are therefore considered to be identical (Fig. 6A,B). In contrast, the photoreceptors of rows 5 and 6 produced narrow spectral sensitivity curves (<100 nm bandwidth), peaking at 565 ± 5 nm ($N=8$, 2 stained – Fig. 6D). The photoreceptors within row 2D also had narrow spectral sensitivity curves peaking at 566 ± 4 nm ($N=6$, 3 stained – Fig. 6C). Row 2D and row 5 and 6 receptors are therefore not only very similar in their polarization sensitivities, but also almost identical in their spectral sensitivities. Their narrow spectral sensitivity curves resemble the narrowly tuned sensitivity curves of colour receptors.

Within row 2, R1, R4 and R5 forming row 2P are sensitive to light, peaking at 600 nm, and they possess lower PS values than row 2D receptors (Table 2). They are therefore clearly grouped with the colour receptors. Within the rhabdoms of the hemispheres and of rows 2D, 5 and 6, the spectral sensitivities of Group I and Group II receptors – which have their microvilli at right angles – were identical.

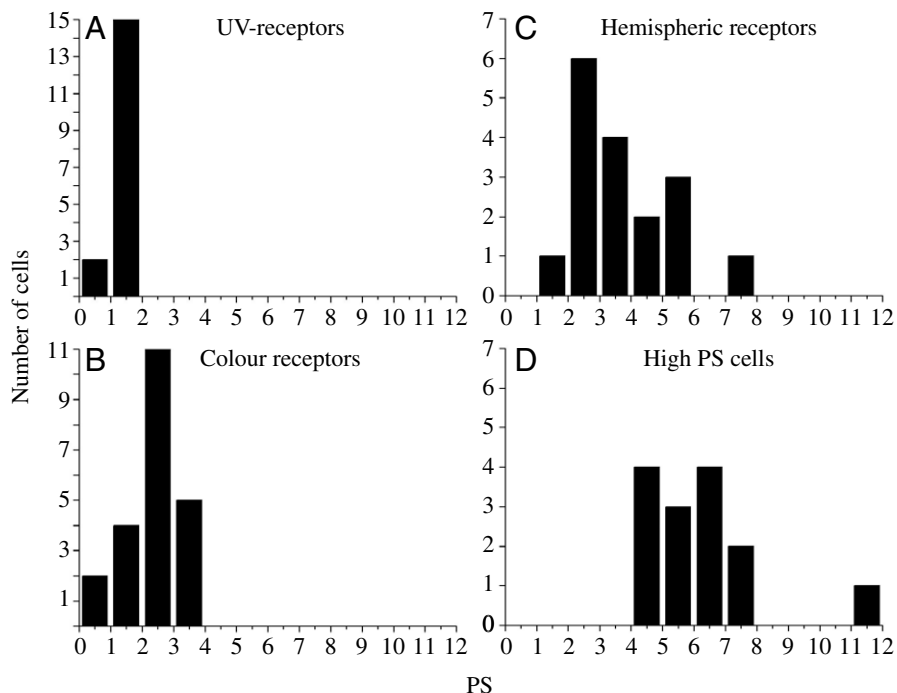


Fig. 5. Histograms of polarization sensitivity values (PS). (A) UV receptors (R8 cells) with PS < 2 ($N=17$); (B) colour receptors within rows 1, 2P, 3, 4 [PS=2.3±2 (s.d.), $N=22$]; (C) hemispheric receptors (ventral and dorsal hemispheres) with a 'typical crustacean' design (PS=3.8±1.6, $N=17$); and (D) 'high PS cells' within rows 2D, 5, 6 (PS=6.1±2, $N=14$). The PS of 'high PS cells' is significantly higher than that of hemispheric receptors (t -test, $P<0.005$).

Directions of maximal sensitivity to the e -vector of polarized light (Φ_{max})

Not surprisingly, the polarization orientations to which photoreceptors were the most sensitive differed by 90° from the orientations to which they were the least sensitive (Fig. 3A,B, Table 1). On the basis of anatomical studies, Marshall et al. (Marshall et al., 1991a) proposed that *Gonodactylus chiragra* possesses four groups of photoreceptors with unidirectional microvilli oriented at +45°, -45°, 90° and 0°. If this hypothesis is right, four Φ_{max} values should be found amongst the polarization-sensitive photoreceptors. Indeed, the electrophysiologically measured Φ_{max} values fall clearly into four groups within ± 5° of the expected Φ_{max} directions (Table 1). Staining of the photoreceptors after recordings confirmed the predictions of Marshall et al. (Marshall et al., 1991a) that each rhabdom contains two populations of cells, Group I and Group II receptors, with mutually perpendicular Φ_{max} values (Fig. 4D). Within the type I rhabdoms of the hemispheres and rows 5 and 6, Group I is formed by three photoreceptors (R1, R4, R5) and Group II by four photoreceptors (R2, R3, R6, R7) (Fig. 2A). The situation in the type II rhabdom of row 2D is, however, different in that the rhabdom consists of only four photoreceptors R2, R3, R6 and R7 (Fig. 2B). However, these receptors are also divided into two groups, R2, R6 and R3, R7, which are sensitive to orthogonal e -vector directions of light (Fig. 4C,D, Table 1). All 'high PS cells' within rows 2D, 5 and 6 and the receptors of the dorsal hemisphere were sensitive to an e -vector of either +45° or -45° relative to the equatorial MB (Table 1). The receptors of the ventral hemisphere were maximally sensitive to an e -vector orientation of 0° or 90°, respectively. Thus, together, the stomatopod's hemispheres

sample four directions of polarized light: +45°, -45°, 0° and 90° (Table 1).

Discussion

Regionalization of polarization sensitivity

In general, the different anatomical structures of photoreceptors from different regions of the stomatopod's apposition compound eye are clearly reflected in their physiology.

Within the structurally unspecialized hemispheric retina, the mean PS values of the photoreceptors R1–R7 (PS=3.8±1.6) are similar to values that have been reported for photoreceptors of the crayfish and the green crab (Glantz, 1996a; Glantz, 1996b; Shaw, 1966; Shaw, 1969; Waterman and Fernandez, 1970). The mean PS value of the stomatopod's 'high PS receptors' is significantly increased (PS=6.1±2). In rows 5 and 6 this may be attributed to the strictly aligned and regularly layered microvilli (Marshall et al., 1991a; Snyder, 1973; Stowe, 1983). Other factors such as fixed orientation of the rhodopsin and its aldehyde group within the microvillus may also play a role but we have no evidence for this. Less expected was the high PS value in photoreceptors of row 2D, because it was believed that all photoreceptors of rows 1–4 are involved in polychromatic colour vision (Cronin and Marshall, 1989b; Marshall et al., 1991b). Confusion is likely to occur between colour and polarization information, and therefore many animals [an exception is the butterfly (Kelber et al., 2001)] structurally destroy PS within their colour receptors (Wehner and Bernard, 1993). Marshall et al. (Marshall et al., 1991a) described orthogonal arrays of microvilli within individual receptors of rows 1–4. Furthermore it was shown that the thickness of the

Table 2. Distribution of polarization sensitivities of R1–R7 cells throughout the retina

Row	Polarization sensitivities									Total
	0–1	1–2	2–3	3–4	4–5	5–6	6–7	7–8	8–13	
1D	1	0	2	1						4
1P		1	1							2
2D					2	0	3	1		6
2P		1	1	2						4
3D			2	1						3
3P		1								1
4D	1	1	3	1						6
4P			2							2
5 and 6					2	3	1	1	1	8
DH			3	2	1	2	0	1		9
VH		1	3	2	1	1				8

orthogonal microvillar layers often varied greatly within these rhabdoms. Both of these morphologies theoretically decrease PS remarkably. Our electrophysiological recordings confirmed these anatomical predictions for the colour receptors (rows 1, 3, 4 and 2P), which did not show appreciable sensitivities to linearly polarized light (2.3 ± 1). However, row 2D was an exception. Re-examination of the ultrastructure of the row 2D rhabdom revealed that single photoreceptors here also possess unidirectional microvilli, which renders them sensitive to linear polarized light. The rhabdom 2D also consists of regular layers of orthogonal microvilli of identical thickness, albeit they are three times thicker than in rows 5 and 6, which may decrease PS due to self-screening (see Fig. 2B). It cannot be determined from our studies if the low PS in 2P receptors is solely due to the structure of the individual receptors or to the filter effect of the distally situated ‘high PS receptors’ within row 2D, which filter out two orthogonal e-vector directions of linearly polarized light ($+45^\circ$, -45°).

Spectral sensitivity of ‘high PS cells’

Spectral sensitivity measurements revealed that all ‘high PS cells’ had similar narrow spectral sensitivity curves (bandwidth <100 nm) peaking at 565 ± 5 nm (Fig. 6C,D). The R1–R7 cells throughout the retina of crayfish are also sensitive to ‘yellow’ light, peaking at 561 nm (Waterman and Fernandez, 1970), although their spectral sensitivity curves are broader than those of the stomatopod’s ‘high PS cells’. The narrow spectral sensitivity curves of ‘high PS cells’ differ from previous microspectrophotometric measurements, where broad spectral absorption spectra were estimated for a variety of gonodactyloid species (Cronin et al., 2002; Cronin and Marshall, 1989a; Cronin et al., 1994a). Electrophysiological measurements are performed on the intact eye, so that filtering effects of all the overlying optical structures are taken into account, whereas microspectrophotometric measurements are from absorbance of excised photoreceptor parts and the estimated spectral sensitivity is based on the photoreceptor and filter lengths alone. Narrow spectral sensitivities have been predicted for row 2D receptors, because of the presence of an intrarhabdomal filter between R8 and row 2D (see Fig. 2)

(Marshall et al., 1991b). No such filters have been described for rows 5 and 6 and the narrow spectral sensitivity curves measured electrophysiologically are a surprise especially in view of the long lengths of the rhabdoms (over $100 \mu\text{m}$). However, it is possible that filtering effects at the level of the R8 cell, the cornea or the crystalline cones exist here.

There are possible reasons for ‘high PS cells’ to be sensitive to yellow light. Water over reefs transmits light best around 550 nm (Jerlov, 1976), which argues for a sensitivity match of the ‘high PS cells’ to the environmental stimulus conditions. Furthermore, the degree to which light is polarized in water is wavelength dependent with a minimum at 450–500 nm (Cronin and Shashar, 2001; Ivanoff and Waterman, 1958; Jerlov, 1976; Shashar et al., 2004). It is therefore useful to position the spectral peaks of polarization receptors on either side of this polarization minimum.

Polarization processing

In general, decapod crustacean rhabdoms possess two groups of polarization receptors sensitive to orthogonal directions of polarized light, which provide separate pathways to the lamina, the first optic ganglion beneath the retina (Eguchi, 1965; Shaw, 1966; Waterman and Fernandez, 1970). Such a dual channel pathway may also exist in *Gonodactylus chiragra*. The determination of Φ_{max} revealed two populations of polarization-sensitive cells within each rhabdom. For clarity we will describe the findings for rows 5 and 6, row 2D and for the hemispheres separately.

In rows 5 and 6 the two populations of polarization-sensitive cells within each rhabdom coincide with the two morphological groupings (Group I and Group II) within the R1–R7 cells. Φ_{max} was found to be at -45° and $+45^\circ$, respectively. The information from each retinula cell group is directed into two separate lamina layers (Kleinlogel and Marshall, 2005; Kleinlogel et al., 2003). Thus separate information channels may exist for linearly polarized light at $+45^\circ$ and -45° with possible antagonistic input to polarization-sensitive interneurons in the medulla.

In contrast, in row 2D the two populations of polarization sensitive cells consist of only two cells each, which belong to

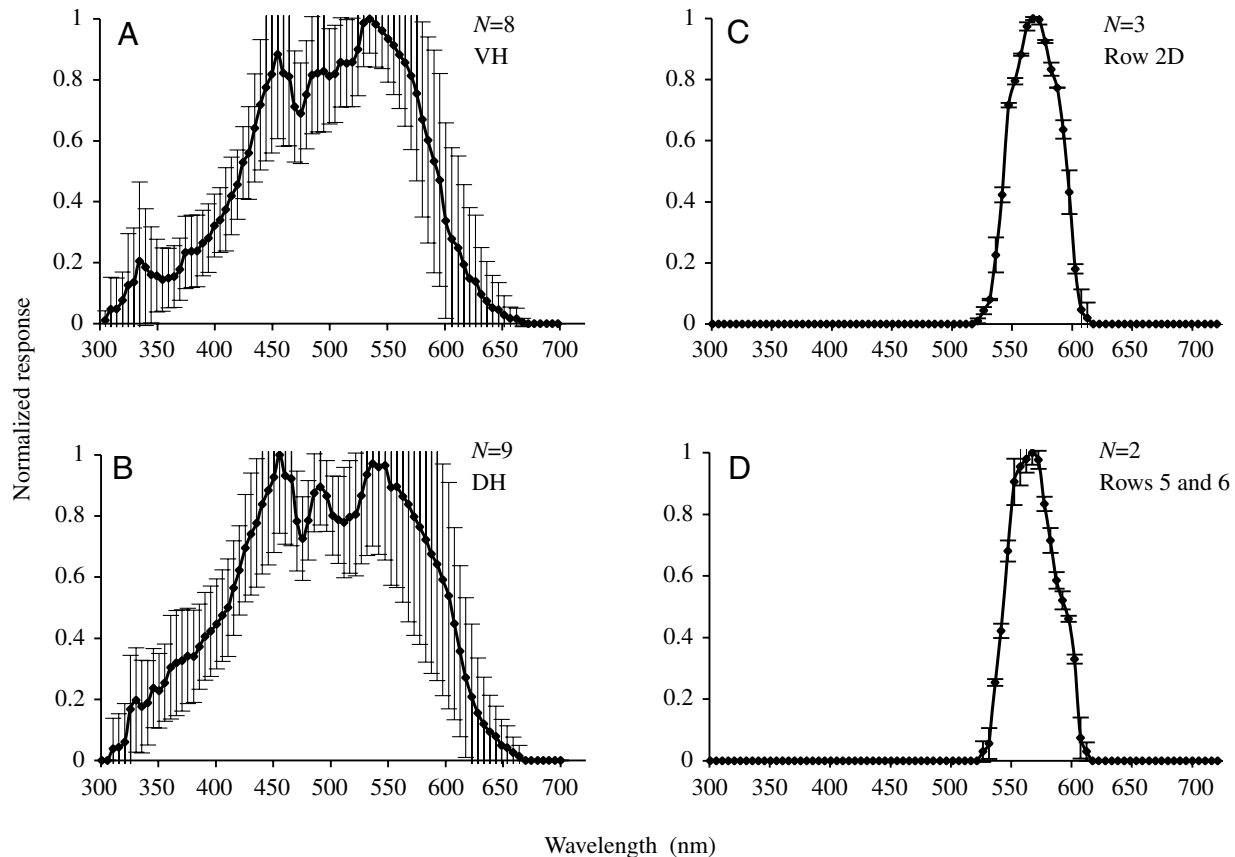


Fig. 6. Averaged spectral sensitivity curves (\pm s.d.) of polarization sensitive photoreceptors from different eye regions in *Gonodactylus chiragra*. Ventral hemisphere (VH; A) and dorsal hemisphere (DH; B) receptors have broad spectral sensitivity curves with two maxima and similar overall sensitivity. The spectral sensitivity curves of 2D receptors (C) and row 5 and 6 receptors (D), which are in this study grouped together as ‘high PS cells’, have very similar, narrow sensitivity curves with a bandwidth of less than 100 nm, peaking at around 565 nm. Only the spectral sensitivities of stained cells were averaged in C and D in order to avoid the incorrect inclusion of a cell with different identity.

the same cell group amongst the R1–R7 cells; R2, R6 and R3, R7. In a right eye, Φ_{\max} for R2 and R6 is at $+45^\circ$ and Φ_{\max} for R3 and R7 is at -45° (Fig. 4D, Table 1). Owing to the fact that the retinula cell arrangement in 2D is symmetrical (Fig. 4C), we currently assume that orthogonal PS information either cancels out within this tier or that it is retained between R2 and R6 *versus* R3 and R7. Two bits of evidence suggest the former is more likely. Firstly, the four photoreceptor axons originating in row 2D all terminate in the same lamina layer and separation of the two orthogonal polarization channels into, for example two sub layers, has not been shown here (Kleinlogel and Marshall, 2005). Secondly, row 2D fits into the scheme of colour sensitivity within stomatopod vision (Cronin and Marshall, 1989a; Cronin and Marshall, 1989b) and high polarization sensitivity within colour receptors is not desirable because of possible confusion of colour with polarization information (Wehner and Bernard, 1993). Clearly we need to know more about the information processing beneath the retina before too much further discussion.

It is worth mentioning that the retinal design of row 2 ommatidia differs from rows 1, 3 and 4 ommatidia in the sense that the cell groups forming the two retinal tiers are inverted

(Marshall et al., 1991a). This cell inversion has no direct effect on the subretinal wiring of photoreceptor axons (Kleinlogel and Marshall, 2005; Kleinlogel et al., 2003), nonetheless, the structural differences may indicate a different function of row 2D beyond the ‘colour vision system’. Since all ‘high PS cells’ are homochromatic, rows 2D, 5 and 6 receptors could potentially subserve the same polarization system without confusing polarization with colour information (Wehner and Bernard, 1993).

Another retinal modification is found in rows 5 and 6. The photoreceptor arrangement in the retina of row 6 is rotated 90° counter-clockwise in relation to row 5 (in a right eye), so that each cell group in row 6 produces microvilli arranged perpendicularly to the ones produced by the same cell group in row 5 (Fig. 4D). Thus the same cell groups of the two rows are sensitive to orthogonal e-vector orientations (Marshall et al., 1991a), but terminate in the identical lamina plexiform layer (Kleinlogel et al., 2003). Here again knowledge of the neural connectivity of photoreceptors is indispensable for interpretation of the above observations with regard to the putative polarization system.

In the dorsal and ventral hemispheres the two populations of

polarization-sensitive cells within each rhabdom also coincide with the two morphological groupings (Group I and Group II) within the R1–R7 cells. In the dorsal hemisphere, Φ_{\max} was found to be at -45° and $+45^\circ$, respectively, whereas in the ventral hemisphere Φ_{\max} was at 0° and 90° , respectively (Table 1). In contrast to other crustaceans examined to date, the retinula cell arrangement in one hemisphere of the eye of *Gonodactylus chiragra* is rotated 45° relative to the other (Marshall et al., 1991a). Consequently the R1–R7 cells within the hemispheric retinas of *Gonodactylus chiragra* sample together four e-vector orientations of polarized light. Most of the ommatidia of the ventral and dorsal hemispheres view the same portion of the visual field and they could therefore provide four information channels for polarized light simultaneously (Marshall and Land, 1993). This would theoretically eliminate neutral points at $\pm 45^\circ$ inherent to a two-dimensional polarization analyser system (Bernard and Wehner, 1977). However, we consider the integration of the polarization channels from the two hemispheres at an early stage of visual processing rather unlikely. This is because the first three visual neuropiles, like the retina, are divided into three areas, one under each hemisphere and one under the MB, which suggests that visual information from the two hemispheres remains isolated and is processed separately (Kleinlogel and Marshall, 2005; Kleinlogel et al., 2003).

Biological significance of polarization vision

The ‘high PS cells’ within the stomatopod’s retina form a linear array of mutually perpendicular e-vector analysers, all of which examine a narrow equatorial strip of the visual scene of 10° diameter (Marshall and Land, 1993). Stomatopods employ vertical scanning eye movements to sweep their linear array of MB receptors over objects of interest. It is believed that these unorthodox eye movements serve the sequential acquisition of colour and polarization information by the specialized MB receptors (Land et al., 1990). They have rotational eye movements too (Land et al., 1990) so that in fact PS relative to the outside world changes continuously. This could potentially remove the ambiguity inherent in having only two preferred e-vector sensitivities (Bernard and Wehner, 1977). Octopus can discriminate e-vector angular differences as low as 20° within a single target and this is possibly facilitated by head or eye movements (Shashar and Cronin, 1996).

Polarization vision under water clearly provides advantages such as contrast enhancement in the scattering environment (Lythgoe, 1971; Lythgoe and Hemmings, 1967; Nilsson, 1996), camouflage breaking of polarization reflective prey (Bernard and Wehner, 1977; Shashar et al., 2000; Shashar et al., 1998) and orientation and navigation in the polarized-light field (Waterman, 1981; Wehner, 2001). Many gonodactyloid stomatopod species, but not *Gonodactylus chiragra*, possess polarization-specific body markings and they may use their ‘high PS cells’ to recognize these remarkable signals displayed by conspecifics in aggressive and mating behaviour (Cronin et al., 2004; Cronin et al., 2003). The use of polarization signals in water is advantageous compared to colour signals because

the colour of objects changes with depth as a result of the varying attenuation across the spectrum, but patterns caused by changes in reflected polarization remain constant (Tyler, 1963; Waterman, 1955). Polarimetric measurements have shown that stomatopod cuticle strongly reflects polarized light in the same waveband that ‘high PS cells’ are sensitive to (Cronin et al., 2003). Moreover, stomatopod cuticle is strongly polarized (50%–70%) compared to the background polarization (30%–50%) and therefore stands out (Cronin et al., 2003). The degree of polarization decreases in water exponentially as a function of distance. Polarization vision is therefore particularly useful for short-range visual tasks, such as communication, without attracting unwanted attention from distant observers (Shashar et al., 2004).

Gonodactylus chiragra is rather exceptional as this species lacks coloured and polarized body markings. They are one of the most restricted species in habitat type, and competition for suitable cavities is therefore intense. It appears that the evolution of lethal weapons for escalated combat rather than body signals for ritualized fighting was more suitable for this species (Caldwell and Dingle, 1976).

List of abbreviations

Colour receptors	photoreceptors of mid-band rows 1, 3, 4 and 2P
D	distal rhabdomal tier
Group I and Group II	subdivision of the R1–R7 cells within an ommatidium
High PS cells	photoreceptors of mid-band rows 2D, 5 and 6
MB	mid-band
P	proximal rhabdomal tier
PS	polarization sensitivity
R1–R8	retinula cells 1–8
Rows 1–6	mid-band rows 1–6
R-log I function	intensity response function
Φ	e-vector orientation of light

We would like to thank Dr T. Labhart, Prof. T. Cronin and Prof. E. Warrant for insightful suggestions, Anthony Chan for the invaluable histological support and Prof. D. Vaney for the generous loan of equipment. We thank Dr J. Douglass, Dr U. Siebeck and Dr M. van Wyk for constructive comments on the manuscript. We would like to acknowledge funding from the American Air Force (AOARD/AFOSR) (FA5209-04-P-0395), the Swiss National Science Foundation (PBSKB–104268/1) and the Australian Research Council (LP0214956).

References

- Bernard, G. D. and Wehner, R. (1977). Functional similarities between polarization vision and color vision. *Vision Res.* **17**, 1019–1028.
- Caldwell, R. L. and Dingle, H. (1976). Stomatopods. *Sci. Am.* **234**, 80–89.
- Cronin, T. W. and Marshall, N. J. (1989a). Multiple spectral classes of photoreceptors in the retinas of gonodactyloid stomatopod crustaceans. *J. Comp. Physiol. A* **166**, 261–275.

- Cronin, T. W. and Marshall, N. J.** (1989b). A retina with at least ten spectral types of photoreceptors in a mantis shrimp. *Nature* **339**, 137-140.
- Cronin, T. W. and Shashar, N.** (2001). The linearly polarized light field in clear, tropical marine waters: spatial and temporal variation of light intensity, degree of polarization and e-vector angle. *J. Exp. Biol.* **204**, 2461-2467.
- Cronin, T. W., Marshall, N. J., Caldwell, R. L. and Shashar, N.** (1994a). Specialisation of retinal function in the compound eyes of mantis shrimps. *Vision Res.* **34**, 2639-2656.
- Cronin, T. W., Marshall, N. J., Quinn, C. A. and King, C. A.** (1994b). Ultraviolet photoreception in mantis shrimp. *Vision Res.* **34**, 1443-1449.
- Cronin, T. W., Caldwell, R. L. and Erdmann, V. E.** (2002). Tuning of photoreceptor function in three mantis shrimp species that inhabit a range of depths. I. Visual pigments. *J. Comp. Physiol. A* **188**, 179-186.
- Cronin, T. W., Shashar, R. L., Caldwell, R. L., Marshall, N., Cheroske, A. G. and Chiou, T.** (2003). Polarization vision and its role in biological signaling. *Integr. Comp. Biol.* **43**, 549-558.
- Cronin, T. W., Shashar, N., Caldwell, R. L., Marshall, J., Cheroske, A. G. and Chiou, T. H.** (2004). Polarization signals in the marine environment. *Proc SPIE* **5158**, 85-92.
- Dacke, M., Nordstroem, P., Scholtz, C. H. and Warrant, E. J.** (2002). A specialized dorsal rim area for polarized light detection in the compound eye of the scarab beetle *Pachysoma sriatum*. *J. Comp. Physiol. A* **188**, 211-216.
- Eguchi, E.** (1965). Rhabdom structure and receptor potential in single crayfish reticular cells. *J. Comp. Physiol.* **66**, 411-429.
- Eguchi, E. and Waterman, T. H.** (1966). Fine structure patterns in crustacean rhabdoms. In *The Functional Organization of the Compound Eye* (ed. C. G. Bernhard), pp. 105-124. Oxford: Pergamon Press.
- Glantz, M. R.** (1996a). Polarization sensitivity in the crayfish lamina monopolar neurons. *J. Comp. Physiol. A* **178**, 413-425.
- Glantz, M. R.** (1996b). Polarization sensitivity in the crayfish optic lobe: Peripheral contributions to opponency and directionally selective motion detection. *J. Neurophys.* **76**, 3404-3414.
- Horváth, G. and Varjú, D.** (2004). *Polarized Light in Animal Vision*. Berlin, Heidelberg, New York: Springer.
- Ivanoff, A. and Waterman, T. H.** (1958). Factors, mainly depth and wavelength, affecting the degree of underwater light polarization. *J. Mar. Res.* **16**, 283-307.
- Jerlov, N. G.** (1976). *Marine Optics*. Amsterdam: Elsevier.
- Kelber, A., Thunell, C. and Arikawa, K.** (2001). Polarisation-dependent colour vision in *Papilio* butterflies. *J. Exp. Biol.* **204**, 2469-2480.
- Kirschfeld, K.** (1973). Vision of polarised light. In *International Biophysics Congress Moscow 4*, pp. 289-296.
- Kleinlogel, S. and Marshall, N.** (2005). Photoreceptor projection and termination pattern in the lamina of gonodactyloid stomatopods (mantis shrimp). *Cell Tissue Res.* **321**, 273-284.
- Kleinlogel, S., Marshall, N. J., Horwood, J. M. and Land, M. F.** (2003). Neuroarchitecture of the color and polarization vision system of the stomatopod *Haptosquilla*. *J. Comp. Neurol.* **467**, 326-342.
- Land, M. F., Marshall, N. J., Brownless, D. and Cronin, T. W.** (1990). The eye movements of the mantis shrimp *Odontodactylus scyllarus* (Crustacea: Stomatopoda). *J. Comp. Physiol. A* **167**, 155-166.
- Lythgoe, J. N.** (1971). Vision. In *Underwater Science* (ed. J. Woods and J. Lythgoe), pp. 103-139. London: Oxford University Press.
- Lythgoe, J. N.** (1979). *The Ecology of Vision*. Oxford: Clarendon Press.
- Lythgoe, J. N. and Hemmings, C. C.** (1967). Polarized light and underwater vision. *Nature* **213**, 893-894.
- Marshall, N. J. and Land, M. F.** (1993). Some optical features of the eyes of stomatopods. I. Eye shape, optical axis and resolution. *J. Comp. Physiol. A* **173**, 565-582.
- Marshall, N. J. and Oberwinkler, J.** (1999). The colourful world of the mantis shrimp. *Nature* **401**, 873-874.
- Marshall, N. J., Land, M. F., King, C. A. and Cronin, T. W.** (1991a). The compound eyes of mantis shrimps (Crustacea, Hoplocarida, Stomatopoda). I. Compound eye structure: the detection of polarised light. *Philos. Trans. R. Soc. Lond. B Biol. Sci.* **334**, 33-56.
- Marshall, N. J., Land, M. F., King, C. A. and Cronin, T. W.** (1991b). The compound eyes of mantis shrimps (Crustacea, Hoplocarida, Stomatopoda). II. Colour pigments in the eyes of stomatopod crustaceans: polychromatic vision by serial and lateral filtering. *Philos. Trans. R. Soc. Lond. B Biol. Sci.* **334**, 57-84.
- Marshall, N. J., Cronin, T. W., Shashar, N. and Land, M.** (1999). Behavioural evidence for polarisation vision in stomatopods reveals a potential channel for communication. *Curr. Biol.* **9**, 755-758.
- Menzel, R.** (1979). Spectral sensitivity and color vision in invertebrates. In *Handbook of Sensory Physiology*. Vol. VII/6A (ed. H. Autrum), pp. 503-580. Berlin, Heidelberg, New York: Springer-Verlag.
- Menzel, R., Ventura, D. F., Hertel, H., de Souza, J. M. and Greggers, U.** (1986). Spectral sensitivity of photoreceptors in insect compound eyes: Comparison of species and methods. *J. Comp. Physiol. A* **158**, 165-177.
- Naka, K. I. and Rushton, W. A. H.** (1966a). S-Potentials from colour units in the retina of fish (Cyprinidae). *J. Physiol.* **185**, 536-555.
- Naka, K. I. and Rushton, W. A. H.** (1966b). S-Potentials from luminosity units in the retina of fish (Cyprinidae). *J. Physiol.* **185**, 587-599.
- Nässel, D. R.** (1976). The retina and retinal projection on the lamina ganglionaris of the crayfish *Pacifastacus leniusculus* Dana. *J. Comp. Neurol.* **167**, 341-360.
- Nilsson, D. E.** (1996). Eye design, vision and invisibility in planktonic invertebrates. In *Zooplankton: Sensory Ecology and Physiology* (ed. P. Lenz, D. Hartline, J. Purcell and D. Macmillan), pp. 149-162. Amsterdam: Gordon & Breach.
- Shashar, N. and Cronin, T. W.** (1996). Polarization contrast vision in *Octopus*. *J. Exp. Biol.* **199**, 999-1004.
- Shashar, N., Hanlon, R. and Petz, A. D.** (1998). Polarization vision helps detect transparent prey. *Nature* **393**, 222-223.
- Shashar, N., Hagan, R., Boal, J. and Hanlon, R.** (2000). Cuttlefish use polarization sensitivity in predation on silvery fish. *Vision Res.* **40**, 71-75.
- Shashar, N., Sabbah, S. and Cronin, T.** (2004). Transmission of linearly polarized light in seawater: implications for polarization signaling. *J. Exp. Biol.* **207**, 3619-3628.
- Shaw, S. R.** (1966). Polarized light responses from crab retinula cells. *Nature* **211**, 92-93.
- Shaw, S. R.** (1969). Sense-cell structure and interspecies comparisons of polarized light absorption in arthropod compound eyes. *Vision Res.* **9**, 1031-1040.
- Snyder, A. W.** (1973). Polarization sensitivity of individual retinula cells. *J. Comp. Physiol.* **83**, 331-360.
- Stowe, S.** (1983). A theoretical explanation of intensity-independent variation of polarisation sensitivity in crustacean retinula cells. *J. Comp. Physiol.* **153**, 435-441.
- Strausfeld, N. J. and Nässel, D. R.** (1981). Neuroarchitecture of brain regions that subserve the compound eyes of crustacea and insects. In *Handbook of Sensory Physiology*. Vol. VII(6) (ed. H. Autrum), pp. 357-344. Berlin, Heidelberg, New York: Springer-Verlag.
- Tyler, J.** (1963). Estimation of percent polarization in deep oceanic water. *J. Mar. Res.* **21**, 102-109.
- Watanabe, A., Obara, S. and Akiyama, T.** (1967). Pacemaker potentials for the periodic burst discharge in the heart ganglion of a stomatopod, *Squilla oratoria*. *J. Gen. Physiol.* **50**, 839-862.
- Waterman, T. H.** (1955). Polarization of scattered sunlight in deep water. In *Papers in Marine Biology and Oceanography*. Vol. 3, pp. 426-434. London: Pergamon.
- Waterman, T. H.** (1966). Information channeling in the crustacean retina. In *Proceedings of the Symposium on Information Processing in Sight Sensory Systems* (ed. P. W. Nye), pp. 48-56. Pasadena: California Institute of Technology.
- Waterman, T. H.** (1981). Polarisation sensitivity. In *Handbook of Sensory Physiology*. Vol. VII/6B (ed. H. Autrum), pp. 283-469. Berlin, Heidelberg, New York: Springer-Verlag.
- Waterman, T. H. and Fernandez, H. R.** (1970). E-Vector and wavelength discrimination by reticular cells of the crayfish *Procambarus*. *Z. Vergl. Physiol.* **68**, 154-174.
- Wehner, R.** (2001). Polarization vision—a uniform sensory capacity? *J. Exp. Biol.* **204**, 2589-2596.
- Wehner, R. and Bernard, G. D.** (1993). Photoreceptor twist: a solution to the false-color problem. *Proc. Natl. Acad. Sci. USA* **90**, 4132-4135.